

The Stability and Dynamics of a Spike in the One-Dimensional Keller-Segel model

K. KANG, T. KOLOKOLNIKOV and M. J. WARD

Kyungkeun Kang, Department of Mathematics, University of British Columbia, Vancouver, Canada V6T 1Z2
Theodore Kolokolnikov, Optique Nonlinéaire Théorique, Université Libre de Bruxelles, Campus de la Plaine, C. P., 231, 1050, Brussels, Belgium (corresponding author)

Michael J. Ward, Department of Mathematics, University of British Columbia, Vancouver, Canada V6T 1Z2

(Draft copy as of June 10th, 2006)

In the limit of a large mass $M \gg 1$, and on a finite interval of length $2L$, an equilibrium spike solution to the classical Keller-Segel chemotaxis model with a linear chemotactic function is constructed asymptotically. By calculating an asymptotic formula for the translational eigenvalue for $M \gg 1$, it is shown that the equilibrium spike solution is unstable to translations of the spike profile. If in addition $L \gg 1$, the equilibrium spike is shown to be metastable as a result of an asymptotically exponentially small eigenvalue. For $M \gg 1$ and $L \gg 1$, an asymptotic ODE for the metastable spike motion is derived that shows that the spike drifts exponentially slowly towards one of the boundaries of the domain. For a certain reduced Keller-Segel model, corresponding to a domain of small length, a solution with a spike at each of the two boundaries is constructed. This solution is found to be metastable, and it is shown that there is an exponentially slow exchange of mass between the two spikes that occurs over very long time scales. For arbitrary initial conditions, energy methods are used to show the global existence of solutions. The relationship between this reduced Keller-Segel model and a Burgers-type equation modeling the upward propagation of a flame-front in a finite channel is emphasized. Full numerical computations are used to confirm the asymptotic results.

1 Introduction

The Keller-Segel model was first introduced in [8] to describe the process of cellular aggregation due to chemotaxis. This model is a PDE system of the

$$u_t = \nabla \cdot (D\nabla u - u\nabla\Phi(v)), \quad v_t = \kappa\Delta v - \gamma v + \alpha u, \quad (1.1)$$

in a domain Ω with no-flux boundary conditions for v and u on the boundary $\partial\Omega$ of Ω . The function $\Phi(v)$ is called the chemotactic function. We will assume a linear such function so that $\Phi(v) = \beta v$. Here D , β , κ , γ , and α , are all positive constants. In this paper we will analyze a singularly perturbed limit of (1.1) in a one-dimensional spatial domain. In dimensionless variables the system (1.1) can be written as (see Appendix A)

$$u_t = u_{xx} - (uv_x)_x, \quad \tau v_t = v_{xx} - v + u, \quad -L < x < L, \quad t > 0. \quad (1.2 a)$$

The three parameters are the domain half-length L , the time-constant τ , and the total mass M defined by

$$M = \int_{-L}^L u \, dx, \quad (1.2 b)$$

which is preserved in time.

There is large body of literature dedicated to (1.2) and its variants in one, two, and higher dimensions. See [6] for an excellent overview. In particular, the two-dimensional version of (1.2) can exhibit a *chemotactic collapse* phenomenon whereby the solution develops a singularity corresponding to a single point blowup at certain points

of the domain in finite time. This collapse process, together with either formal asymptotic or rigorous constructions of the local blowup profile, has been studied by many authors (see [3], [4], [7], [10], and many references in [6]). A certain regularization of the Keller-Segel model, which appears to prohibit blow-up and leads to localized islands of high concentration, was studied in [16] and [17].

In contrast, for the one-dimensional Keller-Segel model (1.2), it has been shown in [10], [12] and [5] that the solution to (1.2) exists globally for all time. In [5] a steady-state solution that consists of a spike at the boundary was also constructed asymptotically. Moreover, numerical experiments in [5] indicate that if an initial condition consists of a spike at some point in the interior of the domain then it will drift towards the boundary.

The first goal of this paper is to study the existence, stability, and dynamics of an equilibrium and a quasi-equilibrium spike solution for (1.2) in the asymptotic limit of a large mass $M \gg 1$. In the limit $M \gg 1$, a spike in u with spatial support of $O(1/M)$ can be constructed asymptotically. Since the domain length is $2L$, we require that $ML \gg 1$. In the limit $M \gg 1$, and with $ML \gg 1$, we first use an asymptotic matching method to construct an equilibrium and a quasi-equilibrium solution for (1.2). For the equilibrium problem, the location x_0 of the spike is at the center of the domain so that $x_0 = 0$. In the limit $M \gg 1$, with $ML \gg 1$, we then study the translational stability of the equilibrium solution by deriving an asymptotic formula for the principal eigenvalue of the linearization. We show that this eigenvalue is positive, and consequently the equilibrium spike is unstable to translations. This result for the eigenvalue supports numerical observations, such as those made in §5 of [5], that a spike that is initially centered near the midpoint of a one-dimensional domain will drift towards the boundary of that domain.

Furthermore, in the dual asymptotic limit of a large mass $M \gg 1$ together with a large domain $L \gg 1$, we show that this translational eigenvalue is positive, but is asymptotically exponentially small. This suggests that a quasi-equilibrium spike solution exhibits metastable behaviour in the limit $M \gg 1$ and $L \gg 1$. We characterize this metastability for $M \gg 1$ and $L \gg 1$ by deriving an asymptotic ODE for the spike location x_0 associated with a quasi-equilibrium solution of (1.2). In the limit, this asymptotic ODE shows that the spike drifts towards one of the boundaries of the domain with an asymptotically exponentially small speed. The analysis of metastability for (1.2) is in the same spirit as previous metastability analyses for other problems (see [18] for a survey), but is rather more intricate owing to the different spatial scales of v and u . More specifically, since u decays rapidly away from a spike for $M \gg 1$, whereas v has a global variation across the domain $[-L, L]$, a straightforward application of a limiting solvability condition, such as was used for related problems in [18], cannot be used here to derive the asymptotic speed of the spike.

The metastable behaviour of localized structures has recently been analyzed for several variants of the Keller-Segel model (1.1). In [13], the effect of volume-filling was analyzed in one spatial dimension whereby the coefficient of the chemotaxis term vanishes at a sufficiently high population density for u . With this model, the chemotaxis term $(uv_x)_x$ in (1.2) is replaced by $(u(1-u)v_x)_x$. In a certain asymptotic limit, this volume-filling Keller-Segel model, which has localized solutions for u in the form of front-back plateau solutions, was shown formally in [13] to exhibit metastable behaviour. In [14] the Keller-Segel model (1.1), under a logarithmic sensitivity function $\Phi(v) = \log(v^p)$, was modified to include a finite rate of increase of v for $u \gg 1$. In a certain asymptotic limit, the resulting model exhibits metastable spike behaviour in both one and two spatial dimensions.

The second goal of this paper is to study the stability of an equilibrium solution, having a boundary spike at each endpoint, to the Keller-Segel model (1.2) in the limit $L \ll 1$ and $ML \gg 1$. This two boundary-spike solution

is marginally unstable, and a certain exponentially small eigenvalue is shown to initiate a metastable competition instability whereby the mass in the two boundary spikes is exchanged exponentially slowly in time until only one of the boundary spikes remain. The study of this phenomena is based on the analysis of a certain *reduced Keller-Segel model*, which is obtained by taking the limit $L \ll 1$ with $ML \gg 1$ in (1.2). The resulting limiting model was first studied in [7] where a certain non-local transformation was used to prove the existence of blowup solutions in two spatial dimensions from a comparison principle. For the corresponding one-dimensional problem we use an analog of this non-local transformation to asymptotically reduce the model (1.2) for $\varepsilon \equiv 2/(ML) \ll 1$ to

$$u_t = \varepsilon u_{xx} - (u_x + 1)v_{xx}, \quad \tau v_t = v_{xx} + u, \quad 0 < x < 2, \quad t > 0; \quad u = v = 0, \quad \text{at } x = 0, 2. \quad (1.3)$$

We remark that the variables u , v , and τ , in (1.3) are not the same as in (1.2) (see §3). For the case $\tau = 0$, (1.2) yields a single equation for u . The resulting equation is of Burgers' type and, rather curiously, also arises in the analysis of [1], [2], [15], and [11], for the upward propagation of a flame-front in a vertical channel. In our context, an asymptotic solution of (1.3) for $\varepsilon \ll 1$ with boundary layers at both endpoints corresponds to the two boundary-spike solution for the Keller-Segel model (1.2) when $L \ll 1$ and $ML \gg 1$. For this class of solution, we extend the metastability analysis of [15] and [11] to the case of the system (1.3) where $\tau > 0$. Our analysis shows that a two boundary-layer solution to (1.3) is unstable due to the presence of an exponentially small positive eigenvalue. This eigenvalue can be interpreted as the initial instability mechanism for the slow mass exchange between two boundary spikes of the Keller-Segel model (1.2) for $L \ll 1$ with $ML \gg 1$.

The final goal of this paper is to give a rigorous proof of the global existence of solutions to (1.3) using energy methods. This analysis complements the analysis of [5] and [10] for the global existence of solutions to the full Keller-Segel model (1.2) in one spatial dimension.

The outline of the paper is as follows. In §2 we construct an equilibrium and a quasi-equilibrium spike solution to (1.2) in limit $M \gg 1$ with $ML \gg 1$. The result is summarized in the (formal) Proposition 1. In this limit, an asymptotic formula for the translational eigenvalue of the equilibrium solution is derived in §2 and summarized in Proposition 2. For $L \gg 1$, this eigenvalue is positive but exponentially small. In Proposition 3 of §2.3 we formally characterize the metastable dynamics of a quasi-equilibrium spike solution by deriving an asymptotic formula for the speed of the spike when $M \gg 1$ and $L \gg 1$. Numerical results are given to confirm both the eigenvalue estimates and the slow spike motion. In §3 we study the metastability of boundary-layer solutions for the reduced Keller-Segel model (1.3). In §4 we prove the global existence of smooth solutions to (1.3). Finally, in §5 we conclude with a brief discussion, and we list a few open problems.

2 Analysis of the Motion of a Spike Solution

In this section we consider a single interior spike solution to (1.2). In §2.1 we begin by formally deriving the asymptotic representation of the spike profile for a quasi-equilibrium spike solution. We then determine the spike location for a true equilibrium solution. The asymptotic result for the quasi-equilibrium solution is given in Proposition 1. For the true equilibrium solution, in Proposition 2 we formally derive an asymptotic formula for the eigenvalue corresponding to an odd eigenfunction. For a large domain length L , this is the eigenvalue associated with a near translation invariance. Since this eigenvalue is positive, the interior equilibrium spike solution is unstable. Finally, in

Proposition 3 of §2.3 we derive an equation of motion for the center of the spike in the special case where the domain length L is asymptotically large.

2.1 The Quasi-Equilibrium Spike Solution

We now summarize the main result of this section in the following formal statement:

Proposition 1 *Consider a one-spike quasi-equilibrium solution of (1.2) with spike location at $x_0 \in (-L, L)$, corresponding to the maximum value of u in $(-L, L)$. Then, for $M \gg 1$ and $ML \gg 1$, u is given by*

$$u \sim \frac{M^2}{8} \operatorname{sech}^2 \left(\frac{M(x - x_0)}{4} \right) + MU_1 + \dots \quad (2.1)$$

For $x - x_0 \leq O(\frac{1}{M})$, the corresponding inner solution for v is

$$v \sim MG(x_0, x_0) - \ln \left[4 \cosh^2 \left(\frac{M(x - x_0)}{4} \right) \right] + \frac{V_1}{M} + \dots \quad (2.2)$$

Alternatively, the outer approximation for v valid for $x - x_0 \gg O(1/M)$ is

$$v \sim MG(x, x_0). \quad (2.3)$$

Here $G(x, x_0)$ is the Green's function satisfying $G_{xx} - G = -\delta(x - x_0)$ with $G_x(\pm L, x_0) = 0$, given explicitly by

$$G(x, x_0) = \frac{1}{\sinh(2L)} \begin{cases} \cosh(x_0 + L) \cosh(x - L), & x_0 < x < L, \\ \cosh(x + L) \cosh(x_0 - L), & -L < x < x_0. \end{cases} \quad (2.4)$$

A leading-order composite expansion v_c for v , which is uniformly valid on $-L \leq x \leq L$, is

$$v_c \sim -\ln \left[4 \cosh^2 \left(\frac{M(x - x_0)}{4} \right) \right] + MG(x, x_0) + \frac{M}{2} |x - x_0|. \quad (2.5)$$

Finally, the true equilibrium solution is obtained when the spike is centered at $x_0 = 0$.

We now derive this result. We assume that u has a spike located at some point $x_0 \in (-L, L)$. In the inner region, where $x - x_0 = O(1/M)$, we introduce the change of variables

$$y = M(x - x_0) \quad u = M^2 U, \quad v = V. \quad (2.6)$$

Substituting (2.6) into the steady-state problem for (1.2) we obtain

$$U'' - (UV')' = 0, \quad V'' - \frac{V}{M^2} + U = 0. \quad (2.7)$$

Here the primes indicate derivatives with respect to y . We then expand

$$U = U_0 + \frac{1}{M} U_1 + \dots, \quad V = MV_c + V_0 + \frac{1}{M} V_1 + \dots, \quad (2.8)$$

where V_c is a constant independent of y to be found. Substituting (2.8) into (2.7), we obtain

$$U_0'' - (U_0 V_0')' = 0, \quad V_0'' + U_0 = 0; \quad U_1'' - (U_0 V_1' + V_0' U_1)' = 0, \quad V_1'' + U_1 = V_c. \quad (2.9)$$

We assume that all of the mass is concentrated in the inner region and so $M = \int_{-L}^L u \, dx$ becomes $\int_{-\infty}^{\infty} U \, dy = 1$. Therefore, $\int_{-\infty}^{\infty} U_0 \, dy = 1$ and $\int_{-\infty}^{\infty} U_j \, dy = 0$ for $j \geq 1$.

Upon imposing $U_0 \rightarrow 0$ as $|y| \rightarrow \infty$ we obtain that $U_0' = U_0 V_0'$. Then, since $\int_{-\infty}^{\infty} U_0 dy = 1$, we obtain from (2.9) for V_0 that U_0 and V_0 satisfy

$$V_0'' + \frac{1}{I_0} e^{V_0} = 0, \quad V_0'(0) = 0; \quad U_0 = \frac{1}{I_0} e^{V_0}, \quad I_0 = \int_{-\infty}^{\infty} e^{V_0} dy. \quad (2.10)$$

In terms of an undetermined constant A , we calculate that $I_0 = 8/A$ and that the solution is

$$V_0(y) = -\ln \left[A \cosh^2 \left(\frac{y}{4} \right) \right], \quad U_0(y) = \frac{1}{8} \operatorname{sech}^2 \left(\frac{y}{4} \right). \quad (2.11)$$

The constants A , and V_c in (2.8), will be found by matching V_0 to the outer solution for v .

From this analysis, it is clear that U_0 decays exponentially to zero as $|y| \rightarrow \infty$ whereas V_0 is linear as $|y| \rightarrow \infty$. Therefore, in the sense of distributions, we can replace the effect of u in the outer region, where $x - x_0 \gg O(1/M)$, by

$$u \rightarrow \left(\int_{-1}^1 u dx \right) \delta(x - x_0) = \frac{1}{M} \left(\int_{-\infty}^{\infty} M^2 \left(U_0 + \frac{1}{M} U_1 + \dots \right) dy \right) \delta(x - x_0) = M \delta(x - x_0). \quad (2.12)$$

In this way, we find that the outer solution for v satisfies

$$v_{xx} - v = -M \delta(x - x_0), \quad v_x(\pm L) = 0. \quad (2.13)$$

In terms of the Green's function $G(x, x_0)$, given explicitly in (2.4), the solution to (2.13) is given in (2.3).

The matching condition for the inner and outer approximations for v is that the far-field behaviour of V as $y \rightarrow \pm\infty$ agrees asymptotically with the behaviour of $G(x, x_0)$ as $x \rightarrow x_0^\pm$. Therefore, we must have

$$M V_c + V_0 + \frac{1}{M} V_1 + \dots \sim M G(x_0, x_0) + G_x(x_0^\pm, x_0) y + G_{xx}(x_0, x_0) \frac{y^2}{2M} + \dots. \quad (2.14)$$

Since $V_0 \sim -\ln(A/4) \mp y/2$ as $y \rightarrow \pm\infty$, as obtained from (2.11), the matching condition (2.14) determines V_c and A as $V_c = G(x_0, x_0)$ and $A = 4$. In addition, this matching condition also shows that the equilibrium location of the spike is the root of $G_x(x_0^+, x_0) = -G_x(x_0^-, x_0)$. Therefore, for the true equilibrium solution we must have $x_0 = 0$. This completes the formal derivation of Proposition 1.

As a remark, we notice that for $L \gg 1$, we have $G_x(x_0^\pm, x_0) = \mp \frac{1}{2} + O(e^{-\gamma L})$ for some γ that depends on x_0 . Therefore, for $L \gg 1$, it is the exponentially small terms in the equilibrium condition $G_x(x_0^+, x_0) = -G_x(x_0^-, x_0)$ that enforce $x_0 = 0$. This exponential ill-conditioning of the equilibrium problem for $L \gg 1$ suggests that the linearization of the true equilibrium solution will have an exponentially small eigenvalue in this limit. This is shown below in §2.2.

For $M = 100$ and $L = 1$, in Fig. 1(a) and Fig. 1(b) we use the asymptotic result in Proposition 1 to plot u and v , respectively, for $x_0 = 0$ and $x_0 = 1/2$. In plotting v in Fig. 1(b) we used the composite expansion v_c given in (2.5). The dashed curves in Fig. 1(b) correspond to the outer solution $v \sim M G(x, x_0)$. Notice that since the inner approximation for v serves only to round a corner layer in the derivative of $G(x, x_0)$ at $x = x_0$, the pointwise values for the outer solution for v and the composite expansion agree rather well over the entire interval.

Finally, we make three remarks. Firstly, since the width of the domain is $O(L)$ while the width of the spike region is $O(1/M)$, the validity of the formal analysis above for $M \gg 1$ also requires that $ML \gg 1$. Secondly, we note that it is possible to change the equilibrium spike location from $x_0 = 0$ to another value by adding a spatially variable term of the form $v_{xx} - a(x)v + u$, for some $a(x) > 0$, in (1.2). For this modification, the leading-order inner solution for u and v are the same as when $a(x) \equiv 1$, except that now the equilibrium spike location would satisfy $G_x(x_0^+, x_0) = -G_x(x_0^-, x_0)$, where $G(x, x_0)$ is the Green's function for $G_{xx} - a(x)G = -\delta(x - x_0)$ with $G_x(\pm L, x_0) = 0$. For this problem $x_0 \neq 0$ in general. Finally, we remark that in §5.1 of [5] a spike profile is constructed asymptotically

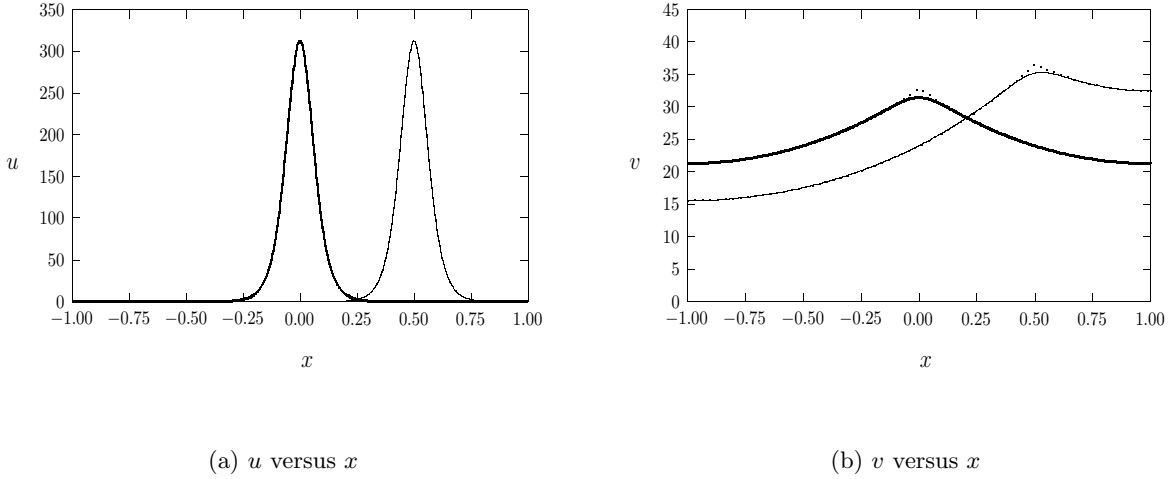


FIGURE 1. The equilibrium and the quasi-equilibrium solution for $M = 100$ and $L = 1$. Left figure: u versus x for $x_0 = 0$ (heavy solid curve) and for $x_0 = 1/2$ (solid curve). Right figure: the composite approximation v_c versus x for $x_0 = 0$ (heavy solid curve) and for $x_0 = 1/2$ (solid curve). The dashed curves in this figure are the outer solutions $v \sim MG(x, x_0)$.

in a different asymptotic limit of the classical Keller-Segel model (1.2). However, formal asymptotic matching was not used in [5] to uniquely determine certain constants in the inner solution.

2.2 Eigenvalue problem

We now determine the stability of the equilibrium spike solution centered at $x_0 = 0$ constructed in §2.1. The equilibrium solution u_e, v_e satisfies

$$u_{xx} - (uv_x)_x = 0, \quad v_{xx} - v + u = 0, \quad |x| < L; \quad u_x(\pm L) = v_x(\pm L) = 0. \quad (2.15)$$

From (2.15), a key relation between u and v is that

$$u_x = uv_x. \quad (2.16)$$

We analyze the stability of this solution by setting

$$u = u_e + e^{\lambda t} \phi(x), \quad v = v_e + e^{\lambda t} \psi(x). \quad (2.17)$$

By substituting (2.17) into (1.2 a) we obtain the following eigenvalue problem on $[-L, L]$:

$$\phi_{xx} - (\phi v_x + u \psi_x)_x = \lambda \phi, \quad \phi_x(\pm L) = 0; \quad \psi_{xx} - (1 + \tau \lambda) \psi = -\phi, \quad \psi_x(\pm L) = 0. \quad (2.18)$$

Below we formally derive an asymptotic formula for the eigenvalue λ of translation in the limit $M \gg 1$ with $ML \gg 1$ and $\lambda \ll M^2$. This eigenvalue is found to be positive, and leads to the translational instability of the spike profile. Our main result is summarized as follows:

Proposition 2 *Consider the one-spike equilibrium solution, centered at $x_0 = 0$, constructed in Proposition 1 in the limit $M \gg 1$ with $ML \gg 1$. In this limit, and assuming that $\lambda \ll M^2$, the translational eigenvalue λ satisfies*

$$\lambda \sim \frac{M}{2} \coth L - \frac{M\mu}{2} \tanh(\mu L), \quad \mu \equiv \sqrt{1 + \tau \lambda}. \quad (2.19)$$

For $\tau = 0$, (2.19) reduces to

$$\lambda \sim \frac{M}{\sinh(2L)}. \quad (2.20)$$

In the limit $L \gg 1$, the solution to the transcendental equation (2.19) satisfies

$$\lambda \sim \frac{2M}{(M\tau/4) + 1} \exp(-2L), \quad L \gg 1. \quad (2.21)$$

Alternatively, in the limit $L \ll 1$, with $ML \gg 1$ and $\tau ML \ll 1$, we obtain

$$\lambda \sim \frac{M}{2L} \left[1 + \frac{ML\tau}{2} \right]^{-1}, \quad L \ll 1, \quad ML \gg 1, \quad \tau ML \ll 1. \quad (2.22)$$

We now derive (2.19). We begin by re-writing (2.18) for ψ as

$$L\psi \equiv \psi_{xx} - \psi + u\psi = \tau\lambda\psi - \phi + u\psi. \quad (2.23)$$

By using $u_x = uv_x$ from (2.16), we obtain upon differentiating the equation for v in (2.15) that $Lv_x = 0$. Then, by using Green's identity on (2.23), together with $v_x = 0$ on $x = \pm L$, we get

$$\tau\lambda \int_{-L}^L v_x \psi dx = - \int_{-L}^L (u_x \psi - \phi v_x) dx - \psi v_{xx}|_{-L}^L. \quad (2.24)$$

We now calculate each of the terms in (2.24). The analysis below shows that ϕ is localized near the spike, while ψ has a significant variation in both the inner region near the spike and in the outer region away from the spike. Therefore, since u is localized near the spike, the dominant contribution to the integral on the right-hand side of (2.24) arises from the spike region where $x = O(M^{-1})$. In contrast, the dominant contribution to the integral on the left-hand side of (2.24) arises from the outer region away from the spike core.

In the inner region where $x = O(M^{-1})$, we introduce the inner variables y , U , V , Φ , and Ψ , defined by

$$y = Mx, \quad u(x) = M^2 U(Mx), \quad v(x) = V(Mx), \quad \phi(x) = M^2 \Phi(Mx), \quad \psi(x) = \Psi(Mx). \quad (2.25)$$

By substituting (2.25) into (2.18), we obtain that $\Phi(y)$ and $\Psi(y)$ satisfy

$$\Phi'' - (\Phi V' + U \Psi')' = \frac{\lambda}{M^2} \Phi, \quad \Psi'' - \frac{\Psi}{M^2} + \Phi = \frac{\tau\lambda}{M^2} \Psi. \quad (2.26)$$

Here the primes indicate derivatives with respect to y . We assume that $\lambda/M^2 \ll 1$, and we expand

$$\Phi = \Phi_0 + \frac{\lambda}{M^2} \Phi_1 + \dots, \quad \Psi = \Psi_0 + \frac{\lambda}{M^2} \Psi_1 + \dots. \quad (2.27)$$

By substituting (2.27) into (2.26), we obtain in terms of the solutions $U(y)$ and $V(y)$ of (2.7) that

$$\Phi_0'' - (\Phi_0 V' + U \Psi_0')' = 0, \quad \Psi_0'' - \frac{\Psi_0}{M^2} + \Phi_0 = 0, \quad (2.28 a)$$

$$\Phi_1'' - (\Phi_1 V' + U \Psi_1')' = \Phi_0, \quad \Psi_1'' - \frac{\Psi_1}{M^2} + \Phi_1 = \tau \Psi_0. \quad (2.28 b)$$

We integrate (2.28 a) for Φ_0 and impose $\Phi_0'(\pm\infty) = \Phi_0(\pm\infty) = 0$. Then, upon using $V' = U'/U$, we get

$$\Phi_0' - \frac{U'}{U} \Phi_0 = U \Psi_0'. \quad (2.29)$$

The solution to (2.29) is

$$\Phi_0 = U \Psi_0. \quad (2.30)$$

Therefore, from (2.28 a), Ψ_0 satisfies

$$\Psi_0'' - \frac{\Psi_0}{M^2} + U\Psi_0 = 0. \quad (2.31)$$

Since $U' = UV'$, we obtain from differentiating (2.7) for V that $\Psi_0 = V'$. Hence, from (2.30), we get

$$\Phi_0 = UV' = U', \quad \Psi_0 = V'. \quad (2.32)$$

Next, we integrate (2.28 b) for Φ_1 and impose $\Phi_1'(\pm\infty) = \Phi_1(\pm\infty) = 0$. By using $V' = U'/U$, we get $(\Phi_1/U)' = \Psi_1' + 1$. Upon integrating this expression and substituting the result into (2.28 b) for Ψ_1 , we get

$$\Phi_1 = U(\Psi_1 + y), \quad (2.33)$$

where Ψ_1 satisfies

$$\Psi_1'' - \frac{\Psi_1}{M^2} + U\Psi_1 = \tau V' - Uy. \quad (2.34)$$

Then, we substitute (2.32) and (2.33) into (2.27), to conclude that

$$\phi = M^2\Phi, \quad \Phi = U\Psi + \frac{\lambda}{M^2}Uy + \dots = U' + \frac{\lambda}{M^2}U(\Psi_1 + y) + \dots. \quad (2.35)$$

Next, we substitute the inner variables (2.25) into the integral on the right-hand side of (2.24). Then, using (2.35), $U' = UV'$, and upon integrating by parts, we obtain

$$\begin{aligned} J &\equiv \int_{-L}^L (u_x\psi - \phi v_x) dx = M^2 \int_{-ML}^{ML} (U'\Psi - \Phi V') dy, \\ &\sim M^2 \int_{-ML}^{ML} \left(U'\Psi - UV'\Psi - \frac{\lambda}{M^2}UV'y \right) dy, \\ &\sim -\lambda \int_{-ML}^{ML} yU' dy = -\lambda \left[yU \Big|_{-ML}^{ML} - \int_{-ML}^{ML} U dy \right]. \end{aligned} \quad (2.36)$$

Since $ML \gg 1$, and $U(\pm\infty) = 0$ with $\int_{-\infty}^{\infty} U dy = 1$ from §2.1, we obtain from (2.36) that

$$J \sim \lambda. \quad (2.37)$$

By substituting (2.37) into (2.24), we get

$$\lambda(\tau I + 1) \sim -\psi v_{xx} \Big|_{-L}^L, \quad I \equiv \int_{-L}^L v_x \psi dx. \quad (2.38)$$

In (2.38) we use the outer approximation for v , which satisfies (2.13) with $x_0 = 0$. Therefore, from (2.3) and (2.4), we obtain that $v_{xx} = v$ at $x = \pm L$ and

$$v(\pm L) \sim \frac{M}{2 \sinh L}, \quad v_x \sim \frac{M}{2 \sinh L} \begin{cases} \sinh(x-L), & 0 < x < L, \\ \sinh(x+L), & -L < x < 0. \end{cases} \quad (2.39)$$

To calculate the outer solution for ψ , we must first represent ϕ in (2.23) in the sense of distributions. A simple calculation shows that for $M \rightarrow \infty$, a localized and odd function of the form $g(Mx)$ can be represented as the dipole distribution $g(Mx) \rightarrow -M^{-2} \left(\int_{-\infty}^{\infty} yg(y) dy \right) \delta'(x)$. Therefore, from (2.35), we have

$$\phi(x) = M^2\Phi(Mx) \quad \rightarrow \quad \left(- \int_{-\infty}^{\infty} yU' dy - \frac{\lambda}{M^2} \int_{-\infty}^{\infty} yU(\Psi_1 + y) dy \right) \delta'(x). \quad (2.40)$$

Since $\lambda/M^2 \ll 1$, we can neglect the second term in (2.40). Then, upon integrating the first term in (2.40) by parts,

and using $\int_{-\infty}^{\infty} U dy = 1$, we obtain that $\phi \rightarrow \delta'(x)$. Therefore, from (2.23), the leading-order outer approximation for ψ satisfies

$$\psi_{xx} - \mu^2 \psi = -\delta'(x), \quad |x| < L; \quad \psi_x(\pm L) = 0; \quad \mu \equiv \sqrt{1 + \tau\lambda}. \quad (2.41)$$

The solution to (2.41) is readily calculated as

$$\psi(\pm L) \sim \mp \frac{1}{2 \cosh(\mu L)}, \quad \psi(x) \sim -\frac{1}{2 \cosh(\mu L)} \begin{cases} \cosh(\mu(x-L)), & 0 < x < L, \\ -\cosh(\mu(x+L)), & -L < x < 0. \end{cases} \quad (2.42)$$

Finally, we substitute (2.39) and (2.42) into (2.38). This yields that

$$\lambda(1 + \tau I) \sim \frac{M}{2 \cosh(\mu L) \sinh(L)}, \quad (2.43)$$

where the integral I in (2.38) is given by

$$I = \frac{M}{2 \sinh L \cosh(\mu L)} \int_0^L \sinh z \cosh(\mu z) dz = \frac{M [\mu \sinh(\mu L) \sinh L - \cosh(\mu L) \cosh L + 1]}{2(\mu^2 - 1) \sinh L \cosh(\mu L)}, \quad (2.44)$$

Substituting (2.44), (2.39), and (2.42) into (2.38), and using $\mu^2 - 1 = \tau\lambda$, we obtain (2.19). This completes the derivation of the formal Proposition 2.

We now show that $\lambda > 0$ from (2.19). To do so, we write (2.19) in the form $F(\lambda) = 0$, where $F(\lambda)$ is defined by

$$F(\lambda) \equiv \lambda + \frac{M\mu}{2} \tanh(\mu L) - \frac{M}{2} \coth L, \quad \mu \equiv \sqrt{1 + \tau\lambda}. \quad (2.45)$$

For any $L > 0$ and $M > 0$, a simple calculation shows that $F(0) < 0$, $F(\lambda) \rightarrow +\infty$ as $\lambda \rightarrow \infty$, and $F'(\lambda) > 0$. Therefore, for any $L > 0$ and $M > 0$, the eigenvalue of translation is unstable. For $M = 100$, and for three values of τ , In Fig. 2(a) we plot the numerical solution to (2.19) as a function of L . For $\tau = 1$, in Fig. 2(b) we plot λ versus L for two values of M . It is easy to show from (2.19) that λ is a decreasing function of τ , a decreasing function of L , and an increasing function of M . In Table 1 we show a largely favorable comparison between the asymptotic result (2.19) for λ and the corresponding full numerical result computed from (2.15) and (2.18). The rather poor agreement for the case $\tau = 1$, $L = 0.5$, and $M = 50$, is improved by increasing M to concentrate the spike near $x = 0$.

From (2.21) we note that the classical Keller-Segel model is exponentially ill-conditioned in the limit $L \gg 1$ and $M \gg 1$. Hence, we expect that the corresponding time-dependent problem will exhibit the phenomena of dynamic metastability in this limit. This is studied in §2.3. Although the eigenvalue estimate (2.19) was done only for the equilibrium solution where $x_0 = 0$, a similar analysis shows that the quasi-equilibrium solution with $x_0 \neq 0$ is also exponentially ill-conditioned when $L \gg 1$ and $M \gg 1$.

2.3 Dynamics

We now derive an equation of motion for the center x_0 of the spike that is valid for $M \gg 1$ and long domains where $L \gg 1$. In this limit, where the eigenvalue was found in §2.2 to be exponentially small, the spike motion is metastable and the spike is found to drift exponentially slowly towards one of the boundaries of the domain.

Proposition 3 *Consider the one-spike quasi-equilibrium solution of Proposition 1 and suppose that $M \gg 1$ and $L \gg 1$. Let $x_0(t)$ be the location of the maximum height of the spike for u at a given time t with $|x_0| < L$. Then, x_0*

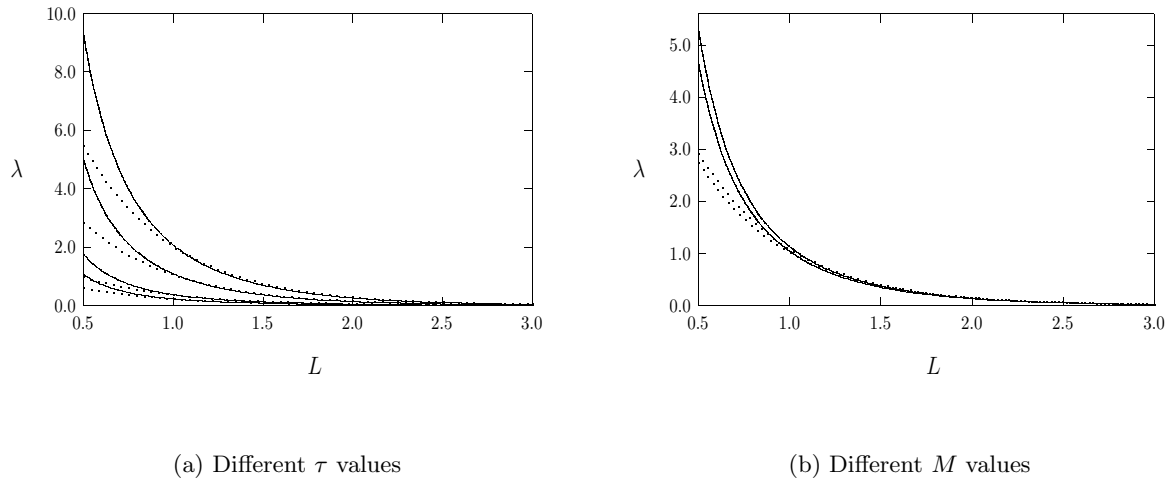


FIGURE 2. Left figure: λ versus L computed numerically with $M = 100$ from (2.19) (solid curves) for $\tau = 0.5$, $\tau = 1.0$, $\tau = 3.0$, and $\tau = 5.0$. At each fixed L , λ increases as τ decreases, and hence the top curve is for $\tau = 0.5$. Right figure: λ versus L computed with $\tau = 1.0$ from (2.19) for $M = 50$ (lower solid curve) and $M = 400$ (upper solid curve). In these figures the dotted curves are the approximations to λ given in (2.21), which are valid for $L \gg 1$.

L	M	τ	$\lambda(\text{full numerics})$	$\lambda(\text{asymptotics})$
0.5	50	0	42.123	42.546
0.5	50	1	7.9095	4.6665
0.5	50	10	1.0997	0.53416
0.5	50	100	0.11527	0.054225
0.5	100	0	85.258	85.092
0.5	100	1	6.0818	5.0144
0.5	100	10	0.66925	0.53862
0.5	100	100	0.067625	0.054271
1	50	0	13.907	13.786
1	50	1	1.3077	1.0364
1	50	5	0.28919	0.22313
1	50	10	0.14658	0.11266
1	50	100	0.014842	0.011366
1	100	0	27.617	27.572
1	100	100	0.012717	0.011371
2	100	1	0.14416	0.13289
3	100	1	0.020318	0.018719
4	100	1	0.0027924	0.0025705
5	50	0	0.0045732	0.00454
5	50	1	0.00040012	0.00033607
5	100	0	0.0090939	0.00908
5	100	1	0.00037919	0.00034899
5	100	100	3.9552e-006	3.6279e-006

Table 1. Comparison of the asymptotic solution for the translation eigenvalue λ given in (2.19) with the corresponding full numerical result computed from (2.15) and (2.18).

satisfies the asymptotic ODE

$$x'_0(t) \sim \exp(-2L) \left[\frac{\tau}{4} + \frac{1}{M} \right]^{-1} \sinh(2x_0). \quad (2.46)$$

We now derive this result. As in §2.1, we introduce the following scalings

$$y = M(x - x_0(t)), \quad u = M^2U, \quad v = V, \quad (2.47)$$

where $U = U(y)$ and $V = V(y)$. We then define σ as the speed of the spike

$$\sigma \equiv x'_0(t). \quad (2.48)$$

Since there is an exponentially small eigenvalue when $L \gg 1$, we assume that $\sigma \ll 1$. Substituting (2.47) and (2.48) into (1.2), we readily derive that

$$U'' - (UV')' = -\frac{\sigma}{M}U', \quad V'' - \frac{V}{M^2} + U = -\frac{\tau\sigma}{M}V'. \quad (2.49)$$

Recall from §2.1 that U is localized near the spike, but that the solution to the leading order problem for V , given by $V'' + U = 0$, does not decay as $y \rightarrow \pm\infty$. Therefore, in order to impose a solvability condition to determine the ODE for $x_0(t)$, we must retain the term $\frac{1}{M^2}V$ in (2.49) to ensure that V decays as $|y| \rightarrow \infty$ when $L \gg 1$.

Next, we expand U and V in terms of $\sigma \ll 1$ as

$$U = U_0 + \sigma U_1 + \dots, \quad V = V_0 + \sigma V_1 + \dots. \quad (2.50)$$

Substituting (2.50) into (2.49) we obtain the following leading-order problem for U_0 and V_0

$$U_0'' - (U_0V_0')' = 0, \quad V_0'' - \frac{V_0}{M^2} + U_0 = 0. \quad (2.51)$$

The system for U_1 and V_1 is

$$U_1'' - (U_0V_1' + U_1V_0')' = -\frac{U_0'}{M}; \quad V_1'' - \frac{V_1}{M^2} + U_1 = -\frac{\tau V_0'}{M}. \quad (2.52)$$

Since $U_0' = U_0V_0'$, we can readily solve for U_1 to obtain

$$U_1 = U_0 \left(V_1 - \frac{y}{M} \right). \quad (2.53)$$

By substituting (2.53) into (2.52), the problem for V_1 becomes

$$LV_1 \equiv V_1'' + U_0V_1 - \frac{V_1}{M^2} = \left(\frac{U_0y}{M} - \frac{\tau V_0'}{M} \right). \quad (2.54)$$

We shall consider (2.54) on the interval $y_- < y < y_+$, where $y_- \equiv -M(L + x_0)$ and $y_+ \equiv M(L - x_0)$. This range corresponds to the entire domain $-L < x < L$.

Although the solution V_0 to (2.51) is exponentially small near $y = y_{\pm}$ when $L \gg 1$, we must include this exponentially small effect in order to derive an accurate ODE for the metastable dynamics. Similar weak boundary effects are essential for a metastability analysis of other problems (cf. [14], [15], [11], and [18]). Therefore, in terms of V_0 and V_1 , the Neumann boundary condition $v_x(\pm L) = 0$ is transformed to the following boundary condition for (2.54):

$$V_1'(y_{\pm}) = -\frac{1}{\sigma}V_0'(y_{\pm}). \quad (2.55)$$

Now as was shown in §2.2, the eigenvalue problem $L\Psi = \lambda\Psi$ with $\Psi' = 0$ at $y = y_{\pm}$ has an exponentially small eigenvalue when $L \gg 1$ and $x_0 = 0$. As remarked in §2.2 this is also true when $x_0 \neq 0$. We then use Green's identity

with Ψ and V_1 on (2.54) and (2.55) to obtain that

$$\lambda \int_{y_-}^{y_+} \Psi v_1 dy - \int_{y_-}^{y_+} \Psi \left(\frac{U_0 y}{M} - \frac{\tau V_0'}{M} \right) dy = \frac{1}{\sigma} \Psi V_0' |_{y_-}^{y_+}. \quad (2.56)$$

From (2.51) it follows that $U_0 \sim ce^{-|y|/2}$ as $y \rightarrow \infty$. Therefore, in the outer region where $y \gg 1$, V_0 satisfies $V_0'' - M^{-2}V_0 \sim 0$, which yields $V_0 \sim ke^{-|y|/M}$. To obtain the constant k in this outer region, we must calculate the effect of U_0 in the equation for V_0 in (2.51) in the sense of distributions. We recall from §2.1 that $u \rightarrow M\delta(x)$ in the outer region. Therefore, $M^2U_0 \rightarrow M\delta(x) = M\delta(y/M) = M^2\delta(y)$, which yields $U_0 \rightarrow \delta(y)$. Thus, in the outer region, the equation for V_0 becomes $V_0'' - \frac{V_0}{M^2} \sim -\delta(y)$. The solution is readily found to be

$$V_0 \sim \frac{M}{2} e^{-|y|/M}. \quad (2.57)$$

As a remark, near $y = y_{\pm} = O(ML)$, V_0 is exponentially small when $L \gg 1$. Therefore, a boundary layer of exponentially small height is required in order for V_0 to satisfy the boundary conditions $V_0'(y_{\pm}) = 0$ exactly. However, this calculation is not needed in our metastability analysis.

Next, we differentiate (2.51) for V_0 with respect to y , and use $U_0' = U_0 V_0'$. By comparing the resulting equation with (2.54) we conclude that $LV_0' = 0$. Therefore, except in a thin boundary layer near the endpoints y_{\pm} , we have $\Psi \sim V_0'$. We use this result together with (2.57) to calculate the second term on the left-hand side of (2.56) as

$$\frac{1}{M} \int_{y_-}^{y_+} \tau \Psi V_0' dy \sim \frac{\tau}{M} \int_{y_-}^{y_+} (V_0')^2 dy \sim \frac{\tau}{4M} \int_{-\infty}^{\infty} e^{-2|y|/M} dy = \frac{\tau}{4}, \quad (2.58 a)$$

$$\frac{1}{M} \int_{y_-}^{y_+} \Psi y U_0 dy \sim \frac{1}{M} \int_{y_-}^{y_+} y V_0' U_0 dy \sim \frac{1}{M} \int_{-\infty}^{\infty} y U_0' dy = -\frac{1}{M}. \quad (2.58 b)$$

In obtaining the last expression in (2.58 b) we used $\int_{-\infty}^{\infty} U_0 dy = 1$ after integrating by parts. Upon substituting (2.58) into (2.56), we obtain

$$\lambda \sigma \int_{y_-}^{y_+} \Psi v_1 dy + \sigma \left(\frac{1}{M} + \frac{\tau}{4} \right) \sim \Psi V_0' |_{y_-}^{y_+}. \quad (2.59)$$

Finally, we must calculate $\Psi(y_{\pm})$. Since $\Psi \sim V_0'$ fails to satisfy the boundary condition $\Psi'(y_{\pm}) = 0$ by exponentially small terms, we must add a boundary layer of exponentially small height near $y = y_{\pm}$ in order to ensure that $\Psi'(y_{\pm}) = 0$. Near $y = y_-$, we have $\Psi'' - \frac{1}{M^2}\Psi \sim 0$. The solution with $\Psi'(y_-) = 0$ is

$$\Psi \sim B \left(e^{-(y-y_-)/M} + e^{(y-y_-)/M} \right), \quad (2.60)$$

for some constant B . To determine B we must have that the growing exponential term in (2.60) agree with $\Psi \sim V_0' \sim \frac{1}{2}e^{y/M}$. This determines B as $B = \frac{1}{2}e^{y_-/M}$. Therefore, we have $\Psi(y_-) \sim 2B$. A similar boundary layer analysis determines $\Psi(y_+)$. In this way, we obtain for $L \gg 1$ that

$$\Psi(y_-) \sim e^{y_-/M} \ll 1, \quad y_- \equiv -M(L + x_0); \quad \Psi(y_+) \sim -e^{-y_+/M} \ll 1, \quad y_+ \equiv M(L - x_0). \quad (2.61)$$

Finally, we use (2.61) and (2.57) to calculate the boundary contribution term in (2.59). Since λ_1 is exponentially small, the integral on the left-hand side of (2.59) is asymptotically smaller than the second term on the left-hand side of (2.59). In this way, we obtain that $\sigma = x_0'$ satisfies the asymptotic ODE

$$\frac{dx_0}{dt} \sim F(x_0) \equiv e^{-2L} \left[\frac{\tau}{4} + \frac{1}{M} \right]^{-1} \sinh(2x_0). \quad (2.62)$$

This completes the derivation of the formal Proposition 3.

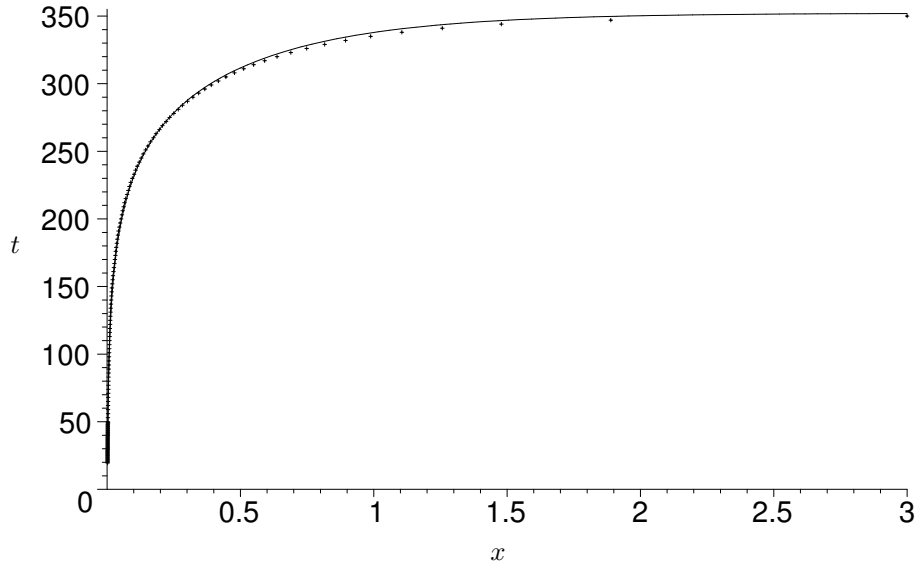


FIGURE 3. Motion of the center of the spike with $M = 100$, $L = 3$, $\tau = 1$. The dotted curve shows the position of the spike as obtained from the full numerical simulation of (1.2). The solid curve is the result obtained from the asymptotic ODE (2.62).

The equilibrium point $x_0 = 0$ of (2.62) is unstable with the asymptotically exponentially small growth rate

$$F'(0) = 2e^{-2L} \left[\frac{\tau}{4} + \frac{1}{M} \right]^{-1}. \quad (2.63)$$

This value is precisely the formula for the exponentially small eigenvalue of Proposition 2 when $L \gg 1$.

In Figure 3 we compare results from the ODE (2.62) with full numerical results for the spike motion computed from (1.2). The initial condition was a one-spike solution with the spike slightly offset from $x_0 = 0$. In the simulation we took $M = 100$, $L = 3$, and $\tau = 1$. Although (2.62) is theoretically valid only when $L \gg 1$, this figure shows that it gives a decent approximation to the full numerical result even for the moderate value of $L = 3$.

3 The Reduced Keller-Segel model

In this section we analyze the reduced Keller-Segel model (1.3). This model was first considered in [7] in the context of analyzing blowup solutions in two spatial dimensions. We begin by deriving (1.3) by taking the limit $L \ll 1$, but with $ML \gg 1$, in (1.2). Introducing $y = x/L$ in (1.2) we get

$$L^2 u_t = u_{yy} - (uv_y)_y, \quad \tau v_t = \frac{1}{L^2} v_{yy} + u - v, \quad 0 < y < 2; \quad \frac{1}{2} \int_0^2 u \, dy = \frac{M}{2L}, \quad (3.1)$$

with $v_y = u_y = 0$ at $y = 0, 2$. Define v_a by $v_a = \frac{1}{2} \int_0^2 v \, dy$. Then, for $L \ll 1$, it follows from (3.1) that $\tau v'_a = M/(2L) - v_a$. Hence, $v_a \rightarrow M/(2L)$ as $t \rightarrow \infty$. This suggests that we make the change of variables

$$v = \frac{M}{2L} (1 + L^2 \mathcal{V}), \quad u = \frac{M}{2L} \mathcal{U}, \quad \tilde{t} = \frac{M}{2L} t. \quad (3.2)$$

By substituting (3.2) into (3.1), we obtain that \mathcal{U} and \mathcal{V} satisfy

$$\mathcal{U}_{\tilde{t}} = \varepsilon \mathcal{U}_{yy} - (\mathcal{U} \mathcal{V}_y)_y, \quad \tilde{\tau} \mathcal{V}_{\tilde{t}} = \mathcal{V}_{yy} + \mathcal{U} - 1 + L^2 \mathcal{V}, \quad 0 < y < 2; \quad \frac{1}{2} \int_0^2 \mathcal{U} \, dy = 1, \quad (3.3)$$

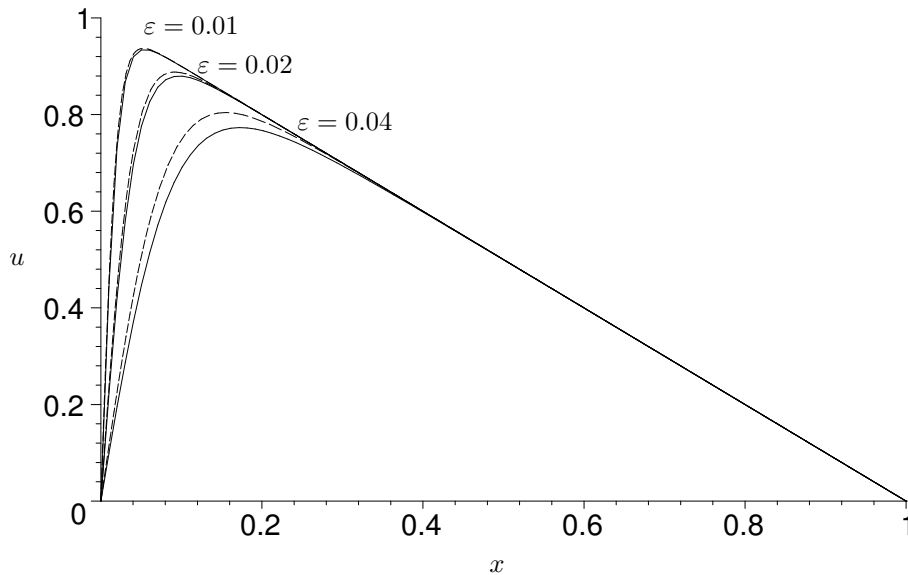


FIGURE 4. The equilibrium solution u to (3.6) on $[0, 1]$ with a boundary layer at $x = 0$. The values of ε are as indicated. The solid and dashed curves are the full numerical and the asymptotic solution (3.7), respectively.

with $\mathcal{U}_y = \mathcal{V}_y = 0$ at $y = 0, 2$. Here ε and $\tilde{\tau}$ are defined by

$$\varepsilon \equiv \frac{2}{ML} \ll 1, \quad \tilde{\tau} = \frac{\tau}{\varepsilon}. \quad (3.4)$$

Since $L \ll 1$, we can neglect the term $L^2\mathcal{V}$ in (3.3). Finally, in (3.5) we introduce \tilde{u} and \tilde{v} defined by

$$\tilde{u} = \int_0^y (\mathcal{U} - 1) ds, \quad \tilde{v} = \int_0^y \mathcal{V} ds. \quad (3.5)$$

In terms of these new variables, and upon replacing y by x and dropping the tilde notation, we obtain that (3.3) transforms to (1.3).

3.1 Equilibrium Boundary-Layer Solutions of the Reduced Model

For $\varepsilon \ll 1$ we now construct certain equilibrium boundary and internal layer solutions to (1.3),

$$\varepsilon u_{xx} - (u_x + 1)v_{xx} = 0, \quad v_{xx} + u = 0, \quad (3.6)$$

with homogeneous Dirichlet boundary conditions for u . This is a standard problem in boundary-layer theory (see section 2.3 of [9]) and the result is summarized formally as follows:

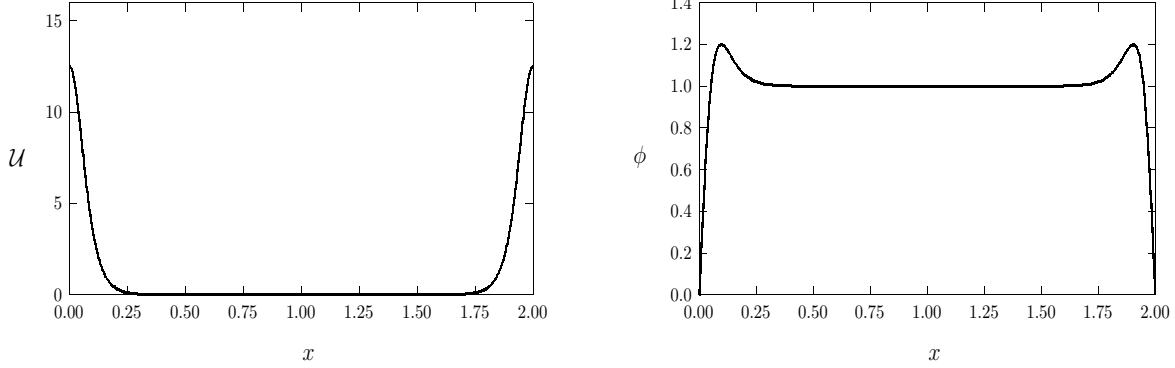
Proposition 4 *With homogeneous Dirichlet boundary conditions, consider the BVP $\varepsilon u_{xx} + (u_x + 1)u = 0$. For $\varepsilon \rightarrow 0$, the following uniformly valid asymptotic equilibrium states are admissible:*

$$u_{b1} \sim \tanh\left(\frac{x}{2\varepsilon}\right) - x, \quad x \in [0, 1]; \quad \text{Single boundary-layer solution on } [0, 1], \quad (3.7)$$

$$u_{i1} \sim \tanh\left(\frac{x}{2\varepsilon}\right) - x, \quad x \in [-1, 1]; \quad \text{Single interior layer solution on } [-1, 1], \quad (3.8)$$

$$u_{b2} \sim \tanh\left(\frac{x}{2\varepsilon}\right) + \tanh\left(\frac{x-2}{2\varepsilon}\right) - x + 1, \quad x \in [0, 2]; \quad \text{Double boundary-layer solution on } [0, 2]. \quad (3.9)$$

For several values of ε , in Fig. 4 we show that the composite expansion (3.7) compares rather favorably with the full numerical solution u to (3.6). In Fig. 5(a) we plot the double boundary-spike solution for \mathcal{U} satisfying (3.3), given by $\mathcal{U} = 1 + u_x$, where u is the double boundary-layer solution u_{b2} for (3.6) given in (3.9).


 (a) \mathcal{U} versus x

 (b) ϕ versus x

FIGURE 5. Left figure: The equilibrium double boundary-spike solution $\mathcal{U} = u_x + 1$ for $\varepsilon = 0.04$, where $u = u_{b2}$ is the double boundary-layer solution given in (3.9). Right figure: the eigenfunction ϕ given in (3.17) on $[0, 1]$ and extended to $[0, 2]$ to be symmetric about $x = 1$.

3.2 Metastability analysis

By performing a stability analysis we now show that the double boundary-layer solution u_{b2} of Proposition 4 is metastable. We linearize around this equilibrium solution by letting $u = u_e(x) + e^{\lambda t}\phi(x)$ and $v = v_e(x) + e^{\lambda t}\psi(x)$. From (1.3), and upon dropping the subscript, we obtain

$$\lambda\phi = \varepsilon\phi_{xx} + u\phi_x - (u_x + 1)\psi_{xx}, \quad \tau\lambda\psi = \psi_{xx} + \phi. \quad (3.10)$$

We then combine the two equations in (3.10) to get

$$\lambda(\phi + (u_x + 1)\tau\psi) = L\phi \equiv \varepsilon\phi_{xx} + (u\phi)_x + \phi. \quad (3.11)$$

Next, we note that for any smooth function w , and with $u(0) = u(1) = 0$, we have Green's identity

$$\int_0^1 wL\phi \, dx = \varepsilon(w_x\phi - w\phi_x)_0^1 + \int_0^1 \phi L^*w \, dx; \quad L^*w \equiv \varepsilon w_{xx} - uw_x + w. \quad (3.12)$$

Here we have formed the inner product over $[0, 1]$ rather than $[0, 2]$, since we can exploit the symmetry of u_{b2} . More specifically, we will look for an even eigenfunction ϕ on $[0, 2]$, which satisfies $\phi_x(1) = 0$. Therefore, we will consider the following boundary conditions on $[0, 1]$:

$$\phi(0) = 0 = \psi(0), \quad \phi_x(1) = 0 = \psi_x(1). \quad (3.13)$$

Let w satisfy $\varepsilon w_x = uw$ on $[0, 1]$. By using u_{b1} in (3.7) we obtain on $[0, 1]$ that

$$w \sim \exp\left(-\frac{x^2}{2\varepsilon}\right) \cosh^2\left(\frac{x}{2\varepsilon}\right), \quad L^*w = (u_x + 1)w \sim \frac{1}{2\varepsilon} \exp\left(-\frac{x^2}{2\varepsilon}\right). \quad (3.14)$$

We note that $w_x(0) = w_x(1) = 0$. We then substitute (3.11), (3.14), and (3.13), into (3.12), to obtain

$$\lambda \int_0^1 [\phi + (u_x + 1)\tau\psi] w dx = -\varepsilon w(0)\phi_x(0) + \int_0^1 \phi(u_x + 1) w dx. \quad (3.15)$$

We now estimate the various terms in (3.15). From (3.11), and assuming that $\lambda \ll 1$, it follows that in the outer region we have $u\phi_x + (u_x + 1)\phi = 0$, which reduces to $(1 - x)\phi_x = 0$. Therefore, for $\varepsilon \ll 1$, ϕ is asymptotically a constant in this region. Without loss of generality, we can impose the normalization condition $\phi(1) = 1$ for ϕ . Hence, $\phi(x) \sim 1$ in the outer region. In the inner region, by rescale $y = \varepsilon^{-1}x$ and $\phi(x) = \Phi(x/\varepsilon)$. Substituting this together with $u \sim U_0(y)$ into (3.11), we obtain the following leading-order equation

$$\Phi'' + (\Phi U_0)' = 0. \quad (3.16)$$

Here the primes indicate derivatives with respect to y . To match to the outer approximation for ϕ , we require that $\Phi(0) = 0$ and $\Phi(\infty) = 1$. The appropriate solution to (3.16) is $\Phi(y) = (yU_0)'$, and hence

$$\phi \sim \frac{d}{dx} \left[x \tanh \left(\frac{x}{2\varepsilon} \right) \right]. \quad (3.17)$$

By using (3.17) together with (3.14) for w we obtain that

$$\varepsilon w(0)\phi_x(0) \sim 1. \quad (3.18)$$

In Fig. 5(b) we plot (3.17) when it is extended to the interval $[0, 2]$ as a symmetric function about $x = 1$.

Next, we decompose (3.15) in terms of three integrals as

$$\lambda(I_1 + \tau I_2) = -1 + I_3. \quad (3.19)$$

Here we have defined

$$I_1 \equiv \int_0^1 \phi w dx, \quad I_2 \equiv \int_0^1 (u_x + 1)\psi w dx, \quad I_3 \equiv \int_0^1 \phi(u_x + 1) w dx. \quad (3.20)$$

To evaluate these integrals, we first establish an identity for $(u_x + 1)w$. We multiply (3.6) by w , and then use the equation $\varepsilon w_x = uw$ for w to readily obtain that $[(u_x + 1)w]_x = 0$. Hence, $(u_x + 1)w = (u_x(0) + 1)w(0)$. We then use (3.7) for u , together with $w(0) = 1$, to establish the identity

$$(u_x + 1)w = \frac{1}{2\varepsilon}, \quad x \in [0, 1]. \quad (3.21)$$

We first evaluate I_3 . By using (3.20), (3.17), and (3.21), we readily calculate that

$$I_3 = \frac{1}{2\varepsilon} \int_0^1 \frac{d}{dx} \left[x \tanh \left(\frac{x}{2\varepsilon} \right) \right] dx = \frac{1}{2\varepsilon}. \quad (3.22)$$

Next, we calculate I_1 . Since w is exponentially large in the outer region, we estimate

$$I_1 \equiv \int_0^1 \phi w \sim \int_0^1 w dx. \quad (3.23)$$

By using (3.14) for w , we calculate in the outer region that

$$w \sim \frac{1}{4} \exp \left(\frac{1}{2\varepsilon} (x^2 - 2x) \right) = \frac{e^{1/(2\varepsilon)}}{4} \exp \left(-\frac{(x-1)^2}{2\varepsilon} \right). \quad (3.24)$$

By substituting (3.24) into (3.23), we calculate that

$$I_1 \sim \frac{e^{1/(2\varepsilon)}}{4} \int_0^1 \exp \left(-\frac{(x-1)^2}{2\varepsilon} \right) dx \sim \frac{\sqrt{\varepsilon}}{4} e^{1/(2\varepsilon)} \int_0^\infty \exp \left(-\frac{z^2}{2} \right) dz = \frac{e^{1/(2\varepsilon)}}{4} \sqrt{\frac{\varepsilon\pi}{2}}. \quad (3.25)$$

Finally, we calculate I_2 . In the outer region we have $\phi \sim 1$. Therefore, assuming that $\lambda\tau \ll 1$, we obtain from (3.10) that $\psi_{xx} \sim -1$, with $\psi(0) = 0$ and $\psi_x(1) = 0$. The solution is $\psi \sim x - x^2/2$. Therefore, we have that

$$I_2 \sim \int_0^1 \frac{1}{2\varepsilon} \left(x - \frac{x^2}{2} \right) dx = \frac{1}{6\varepsilon}. \quad (3.26)$$

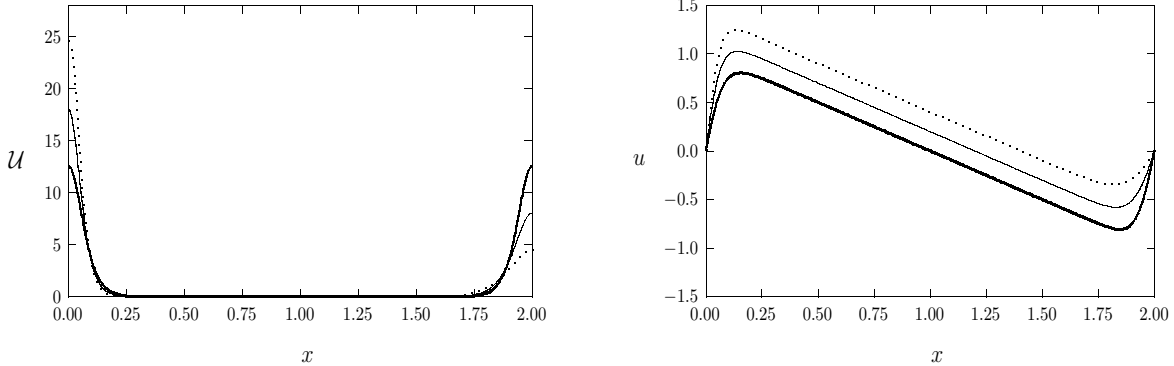
Upon substituting (3.22), (3.25), and (3.26), into (3.19), we obtain that

$$\lambda \left(\frac{e^{1/(2\varepsilon)}}{4} \sqrt{\frac{\varepsilon\pi}{2}} + \frac{\tau}{6\varepsilon} \right) \sim \frac{1}{2\varepsilon} - 1. \quad (3.27)$$

For $\tau \ll O(\sqrt{\varepsilon}e^{1/(2\varepsilon)})$, we can extract the dominant terms in (3.27) for $\varepsilon \ll 1$ to obtain the next main result:

Proposition 5 *Suppose that $\tau \ll O(\sqrt{\varepsilon}e^{1/(2\varepsilon)})$ and $\varepsilon \ll 1$. Then the double boundary-layer solution u_{b2} of Proposition 4 is unstable with respect to an even perturbation. The corresponding eigenvalue λ is exponentially small and*

$$\lambda \sim 2 \exp\left(-\frac{1}{2\varepsilon}\right) \sqrt{\frac{2}{\pi\varepsilon^3}} \left(1 - \frac{2\tau}{3} \exp\left(-\frac{1}{2\varepsilon}\right) \sqrt{\frac{2}{\pi\varepsilon^3}} + O(\varepsilon) \right). \quad (3.28)$$



(a) \mathcal{U} versus x

(b) u versus x

FIGURE 6. Left figure: the slow dynamics of the quasi-equilibrium double boundary-spike solution $\mathcal{U} = u_x + 1$ in (3.30) showing the slow exchange of mass between the two boundary spikes for $\varepsilon = 0.04$. Since $x_0(0) = 1.01 > 1$, the left spike has an initial mass slightly larger than the right spike. Right figure: the double boundary-layer solution u in (3.29). In these figures, the heavy solid curves are for $t = 0$, the solid curves are for $t = 3.2845 \times 10^4$ and $x_0 = 1.2$, and the dashed curve is for $t = 3.3541 \times 10^4$ and $x_0 = 1.4$. Eventually the right spike loses all its mass to the left one.

Note that the relative error term in this expansion is $O(\varepsilon)$ and it swamps the exponentially small correction due to τ . The $O(\varepsilon)$ error comes from a poor estimate of $\int_0^1 w dx$. To obtain a better estimate, it is necessary to compute w to a higher order, which would involve the computation of higher order corrections for the equilibrium solution. Nevertheless, Proposition 5 shows the instability of a double boundary-layer solution. As a numerical example, with $\varepsilon = 0.05$ we obtain from a full numerical computation that $\lambda = 0.007223381$ when $\tau = 0$. This compares well with the asymptotic prediction of $\lambda \sim 0.006479929$. Next, for $\tau = 1$ we obtain $\lambda = 0.00720314197261$ so that $\frac{\lambda|_{\tau=0} - \lambda|_{\tau=1}}{\lambda|_{\tau=0}} = 0.0028$. This compares favorably with the theoretical prediction of $\frac{2}{3} \exp\left(-\frac{1}{2\varepsilon}\right) \sqrt{\frac{2}{\pi\varepsilon^3}} = 0.0021$.

Remark 6 *The equilibrium problem (3.6) for u for the reduced Keller-Segel model (1.3) also arises in the analysis of [1], [2], [15], and [11], for the upward propagation of a metastable flame-front in a vertical channel. The time-dependent flame-front problem is equivalent to (1.3) for the case $\tau = 0$. The eigenvalue estimate in (3.28) for $\tau = 0$ agrees with the asymptotic estimate given in equation (3.29) of [11], which was derived by first transforming (1.3) with $\tau = 0$ to a quasi-linear problem (see §1 of [11]). The analysis here leading to an estimate of λ , corrects an error made in the eigenvalue calculation of equation (3.27) of [15], resulting from an incorrect evaluation of one integral.*

Finally, we discuss quasi-equilibrium double boundary-layer solutions u to (3.6) given by

$$u = x_0 \tanh\left(\frac{x_0 x}{2\varepsilon}\right) - (2 - x_0) \tanh\left(\frac{(2 - x_0)(2 - x)}{2\varepsilon}\right) + (2 - x_0) - x. \quad (3.29)$$

In the outer region, $u \sim x_0 - x$. The double boundary-spike solution \mathcal{U} to (3.3), given by $\mathcal{U} = u_x + 1$, is

$$\mathcal{U} = \frac{x_0^2}{2\varepsilon} \operatorname{sech}^2\left(\frac{x_0 x}{2\varepsilon}\right) + \frac{(2 - x_0)^2}{2\varepsilon} \operatorname{sech}^2\left(\frac{(2 - x_0)(2 - x)}{2\varepsilon}\right). \quad (3.30)$$

From (3.30), the left boundary spike has more mass than the right one when $x_0 > 1$. Then, the slow dynamics of x_0 characterizes the slow mass exchange between the two spikes. For $\tau \ll 1$, we obtain from §3.2 of [11] (see also Corollary 2 of [15]) that $x_0(t)$ satisfies the asymptotic ODE

$$x_0' \sim \sqrt{\frac{2}{\pi\varepsilon}} \left[(2 - x_0)^2 e^{-(2 - x_0)^2/2\varepsilon} - x_0^2 e^{-x_0^2/2\varepsilon} \right]. \quad (3.31)$$

In Fig. 6 we illustrate this slow mass exchange mechanism for the case where $x_0(0) = 1.01$, for which $x_0' > 0$. In this case, the right boundary spike in \mathcal{U} will disappear at some finite time.

4 Global Solution to a Reduced Model

In this section we give a simple proof that solutions to the *reduced* Keller-Segel model (1.3) exist globally in time. With primes denoting partial derivatives with respect to x , we first re-write (1.3) as

$$u_t = \varepsilon u'' - (1 + u')v'', \quad \tau v_t = v'' + u, \quad \text{in } \Omega \times I = [-1, 1] \times [0, T]. \quad (4.1)$$

For (4.1), the following initial conditions and Dirichlet boundary conditions are assumed

$$u(\cdot, 0) = u_0(x), \quad v(\cdot, 0) = v_0(x); \quad u(\cdot, t) = v(\cdot, t) = 0 \quad \text{at } x = \pm 1. \quad (4.2)$$

We summarize our main result as follows:

Proposition 7 *Let u and v be solutions to the reduced Keller-Segel model (4.1) and (4.2). If $u_0(x)$ and $v_0(x)$ are smooth, then u and v are smooth for all time.*

Proof Without loss of generality we can assume for simplicity that $\varepsilon = 1$ and $\tau = 1$, since different values of these parameters do not affect our analysis regarding global existence. We first note that u and v are uniformly bounded from the formulation of the solutions in (3.5). We also note that we can use a standard estimate for a linear parabolic equation to derive that v in (4.1) satisfies

$$\|v_t\|_{L_x^p, L_t^q(\Omega \times I)} + \|v\|_{W_x^{2,p}, L_t^q(\Omega \times I)} \leq C \|u\|_{L_x^p, L_t^q(\Omega \times I)}, \quad (4.3)$$

for any $1 < p, q < \infty$. Here $\|f\|_{L_x^p, L_t^q}$ indicates the mixed norm of L^p and L^q in space and time variables for a measurable function f , namely $\|f\|_{L_x^p, L_t^q(\Omega \times I)}^q = \int_I \|f(\cdot, t)\|_{L^p(\Omega)}^q dt$. In (4.3) we have denoted by $W^{k,p}$ the usual Sobolev space for the case where all derivatives up to the k^{th} order are in L^p . We remark that since u is uniformly bounded and Ω is a bounded domain, the right-hand side of (4.3) is bounded by a fixed constant depending on p, q and T . Next, we obtain $u_t' = u''' - [(u' + 1)v'']'$, upon differentiating the first equation in (4.1) with respect to x . Multiplying this equation by u' , and integrating the resulting equation by parts, we readily obtain

$$\frac{1}{2} \frac{d}{dt} \int_{\Omega} |u'|^2 dx + \int_{\Omega} |u''|^2 dx = \int_{\Omega} (u' + 1)v''u'' dx. \quad (4.4)$$

Here we have used that $u'' = 0$ and $v'' = 0$ at the boundaries $x = \pm 1$.

We need to estimate the right-hand side in (4.4). To do so, we re-write it as follows:

$$\int_{\Omega} (u' + 1)v''u'' dx = \int_{\Omega} u'v''u'' dx + \int_{\Omega} v''u'' dx := I + II. \quad (4.5)$$

Due to standard interpolations of Sobolev norms, we have the following estimates:

$$\begin{aligned} \|u'\|_{L^2(\Omega)} &\leq C \|u\|_{L^2(\Omega)}^{\frac{1}{2}} \|u''\|_{L^2(\Omega)}^{\frac{1}{2}}, \\ \|u\|_{L^4(\Omega)} &\leq C \|u\|_{L^2(\Omega)}^{\frac{3}{4}} \|u'\|_{L^2(\Omega)}^{\frac{1}{4}}, \\ \|u'\|_{L^4(\Omega)} &\leq C \|u'\|_{L^2(\Omega)}^{\frac{3}{4}} \|u''\|_{L^2(\Omega)}^{\frac{1}{4}}. \end{aligned}$$

Here we have used the facts that $u = 0$ on the boundary and that the average of u' is zero. By using these estimates, together with the Hölder inequality, we obtain for the first term I in (4.5) that

$$I = \int_{\Omega} u'v''u'' dx \leq \|u'\|_{L^4(\Omega)} \|v''\|_{L^4(\Omega)} \|u''\|_{L^2(\Omega)} \leq C \|u\|_{L^2(\Omega)}^{\frac{3}{8}} \|v''\|_{L^4(\Omega)} \|u''\|_{L^2(\Omega)}^{\frac{13}{8}}.$$

Then, since u is bounded and Ω is a bounded domain, we obtain

$$I \leq C \|v''\|_{L^4(\Omega)} \|u''\|_{L^2(\Omega)}^{\frac{13}{8}} \leq C \|v''\|_{L^4(\Omega)}^{\frac{16}{3}} + \frac{1}{4} \|u''\|_{L^2(\Omega)}^2.$$

Here we have used Young's inequality in the last inequality above. For the second term II in (4.5), we estimate

$$II \leq \|v''\|_{L^2(\Omega)} \|u''\|_{L^2(\Omega)} \leq C \|v''\|_{L^2(\Omega)}^2 + \frac{1}{4} \|u''\|_{L^2(\Omega)}^2.$$

In summary, by using the estimate (4.3) together with the other estimates above, we conclude that

$$\begin{aligned} \int_{\Omega} |u'(\cdot, T)|^2 dx + \int_0^T \int_{\Omega} |u''|^2 dx dt &\leq \int_{\Omega} |u'(\cdot, 0)|^2 dx + C \int_0^T \int_{\Omega} |v''|^2 dx dt + C \int_0^T \left(\int_{\Omega} |v''|^4 dx \right)^{\frac{4}{3}} dt \\ &\leq \int_{\Omega} |u'(\cdot, 0)|^2 dx + C \int_0^T \int_{\Omega} |u|^2 dx dt + C \int_0^T \left(\int_{\Omega} |u|^4 dx \right)^{\frac{4}{3}} dt \leq \int_{\Omega} |u'(\cdot, 0)|^2 dx + CT. \end{aligned}$$

Here we have used that u is bounded. From this final estimate we conclude that u is continuous by the Sobolev embedding argument. Therefore, by a standard bootstrap procedure, it follows that u and v are smooth. \blacksquare

Remark 8 For the case $\tau = 0$, where the chemotactic equation is of elliptic type, we can also show that solutions to (4.1) are smooth. This case, in fact, is much simpler to treat than the case where $\tau > 0$, and so we leave the details to the reader. Indeed, if $\tau = 0$, then the system (4.1) can be reduced to $u_t = u'' + (1 + u')u$. By following a similar procedure as for case where $\tau > 0$, we can again show that u , and consequently v , are both smooth.

5 Conclusion

In a one-dimensional domain, and in the asymptotic limit of a large mass $M \gg 1$, a quasi-equilibrium spike solution for the classical Keller-Segel model with a linear chemotactic function was constructed. In this limit, the equilibrium spike solution was found to be translationally unstable, and is metastable for asymptotically large domain lengths L . For $M \gg 1$ and $L \gg 1$, an asymptotic ODE for the metastable spike motion was derived that showed that the spike drifts exponentially slowly towards one of the boundaries of the domain. For $L \gg 1$ and $M \gg 1$, the existence of an exponentially small eigenvalue indicates that the solution to the classical Keller-Segel model can be highly sensitive to small perturbations. This sensitivity for $M \gg 1$ and $L \gg 1$ suggests a strong lack of robustness in biological modeling based on the classical Keller-Segel model, and it also suggests that severe difficulties will be encountered in trying to numerically compute solutions. In contrast, for $M \gg 1$ and $L = O(1)$, the translation eigenvalue is unstable, but not exponentially small. In this parameter range, it would be interesting to construct a traveling-wave spike solution to characterize the motion of the spike.

For a reduced Keller-Segel model (1.3) we have studied the stability of an equilibrium solution that consists of two boundary spikes centered at the endpoints of the domain. Rather curiously, the equilibria of this reduced Keller-Segel model are very similar to those of the model of [1], [2], [15], and [11], for the upward propagation of a flame-front in a vertical channel. We showed that this double boundary-spike solution to the reduced Keller-Segel model is unstable due to an asymptotically exponentially small positive eigenvalue in the spectrum of the linearized problem. This eigenvalue is estimated precisely. The shape of the corresponding eigenfunction is shown to initiate an exchange of mass between the two boundary spikes in such a way that after a very long time one of the two boundary spikes fully absorbs the mass of the other. Finally, we have shown that solutions to the *reduced* Keller-Segel model with arbitrary initial conditions exist globally in time.

There are several open problems related to this study. The first open problem is to extend the derivation of the equations of motion of the center of the spike (2.46) to the case when the domain length L is not large. The second issue concerns the stability of a homoclinic stripe solution of zero curvature to the Keller-Segel model in a square domain under a linear chemotactic function. For this two-dimensional problem, it would be interesting to determine if spot-generating breakup instabilities of the stripe can occur, and if so, whether they are the precursor to a finite-time blow-up of solutions to the Keller-Segel model. A third open problem is to analyze the existence and stability of spike solutions to a modified Keller-Segel model in two space dimensions, where the rate of increase of v with respect to u saturates as $u \rightarrow \infty$. In a certain asymptotic limit, this saturation effect was shown to lead to metastable spikes for the two-dimensional Keller-Segel model under a logarithmic chemotactic function $\Phi(v) = \ln v^p$ in (1.1). It would be interesting to extend that analysis to the case of a linear chemotactic function.

Acknowledgements

M. J. W. was supported by NSERC (Canada) under grant 81541, T. K. was partially supported by an NSERC Postgraduate Fellowship, and K. Kang was supported by a PIMS Postgraduate Fellowship. M. J. W. is grateful to Prof. Ricardo Carretero (SDSU) and Prof. Robert Russell (SFU) for preliminary numerical experiments suggesting the possibility of metastability in the Keller-Segel model.

Appendix A Nondimensionalization of the Keller-Segel Model

We consider (1.1) for U, V , with $\Phi(V) = \beta V$, in the one-dimensional domain $-\mathcal{L} < X < \mathcal{L}$ given by

$$U_T = DU_{XX} - \beta(UV_X)_X, \quad V_T = \kappa V_{XX} - \gamma V + \alpha U. \quad (\text{A.1})$$

The total mass is given by $\int_{-\mathcal{L}}^{\mathcal{L}} U dX = \mathcal{M}$. We introduce the non-dimensional variables u, v, x , and t , by

$$T = \omega t, \quad U = U_0 u, \quad V = V_0 v, \quad X = L_d x. \quad (\text{A.2})$$

In terms of these variables, (A.1) becomes

$$\frac{L_d^2}{D\omega} u_t = u_{xx} - \frac{\beta V_0}{D} (uv_x)_x, \quad \frac{1}{\gamma\omega} v_t = \frac{\kappa}{L_d^2 \gamma} v_{xx} - v + \frac{\alpha U_0}{\gamma V_0} u, \quad (\text{A.3})$$

on the domain $|x| < L \equiv \mathcal{L}/L_d$. This form suggests the choices

$$\omega = \frac{\kappa}{D\gamma}, \quad L_d = \sqrt{\frac{\kappa}{\gamma}}, \quad V_0 = \frac{D}{\beta}, \quad U_0 = \frac{D\gamma}{\alpha\beta}. \quad (\text{A.4})$$

In addition, the mass condition $\int_{-\mathcal{L}}^{\mathcal{L}} U dX = \mathcal{M}$ transforms to $\int_{-L}^L u dx = \mathcal{M}/(U_0 L_d)$. In this way, we obtain (1.2) with the three nondimensional parameters τ, L , and M , defined by

$$\tau \equiv \frac{D}{\kappa}, \quad L \equiv \mathcal{L} \sqrt{\frac{\gamma}{\kappa}}, \quad M \equiv \frac{M\alpha\beta}{D\sqrt{\gamma\kappa}}. \quad (\text{A.5})$$

Therefore, the limit $L = O(1)$ and $M \gg 1$ can be interpreted as D small with κ fixed, or equivalently β is large relative to the other parameters. The limit $L \gg 1$ and $M \gg 1$, where metastability occurs, is when both D and κ are small relative to the other parameters.

References

- [1] H. Berestycki, S. Kamin, G. Sivashinsky, *Nonlinear Dynamics and Metastability in a Burgers-Type Equation*, Comptes Rendus Acad. Sci., Paris t., **321**, Sérié 1, (1995), pp. 185–190.
- [2] H. Berestycki, S. Kamin, G. Sivashinsky, *Metastability in a Flame Front Evolution Equation*, Interfaces and Free Boundaries, **3**, (2001), pp. 361–392.
- [3] S. Childress, J. Percus, *Nonlinear Aspects of Chemotaxis*, Math Biosciences, **56**, (1981), pp. 217–237.
- [4] M. A. Herrero, J. J. L. Velázquez, *Chemotactic Collapse for the Keller-Segel Model*, J. Math. Biol., **35**, (1996), pp. 583–623.
- [5] T. Hillen, A. Potapov, *The One-Dimensional Chemotaxis Model: Global Existence and Asymptotic Profile*, Math. Meth. Appl. Sci., **27**, (2004), pp. 1783–1801.
- [6] D. Horstmann, *From 1970 Until Present: The Keller-Segel Model in Chemotaxis and its Consequences*, I. Jahresber. Deutsch. Math.-Verein., **105**(3), (2003), pp. 103–165.
- [7] W. Jäger, S. Luckhaus, *On Explosions of Solutions to a System of Partial Differential Equations Modelling Chemotaxis*, Trans. Am. Math. Soc., **329**, No. 2, (1992), pp. 819–824.
- [8] E. F. Keller, L. A. Segel, *Model for Chemotaxis*, J. Theor. Biol., **30**, (1971), pp. 225–234.
- [9] J. Kevorkian, J. Cole, *Multiple Scale and Singular Perturbation Methods*, Applied Mathematical Sciences, Vol. 114, Springer-Verlag, New York, (1996).
- [10] T. Nagai, *Blow-up of Radially Symmetric Solutions to a Chemotaxis System*, Adv. Math. Sci. Appl., **5**, (1995), pp. 581–601.
- [11] C. Ou, M. J. Ward, *A Metastable Flame-Front Interface and Carrier's Problem*, J. Comput. Appl. Math., **190**, No. 1-2, (2006), pp. 354–371.
- [12] K. Osaki, A. Yagi, *Finite Dimensional Attractors for One-Dimensional Keller-Segel Equations*, Funkcialaj Ekvacioj, **44**, (2001), pp. 441–469.
- [13] A. Potapov, T. Hillen, *Metastability in Chemotaxis Models*, J. Dynam. Differential Equations, **17**, No. 2, (2005), pp. 293–330.
- [14] B. D. Sleeman, M. J. Ward, J. C. Wei, *The Existence, Stability, and Dynamics of Spike Patterns in a Chemotaxis Model*, SIAM J. Appl. Math., **65**, No. 3, (2005), pp. 790–817.

- [15] X. Sun, M. J. Ward, *Metastability for a Generalized Burgers Equation with Applications to Propagating Flame-Fronts*, European J. Appl. Math., **10**, No. 1, (1999), pp. 27–53.
- [16] J. J. L. Velazquez, *Point Dynamics in a Singular Limit of the Keller-Segel Model 1: Motion of the Concentration Regions*, SIAM J. Appl. Math., **64**, No. 4, (2004), pp. 1198–1223.
- [17] J. J. L. Velazquez, *Point Dynamics in a Singular Limit of the Keller-Segel Model 1: Formation of the Concentration Regions*, SIAM J. Appl. Math., **64**, No. 4, (2004), pp. 1224–1248.
- [18] M. J. Ward, *Exponential Asymptotics and Convection-Diffusion-Reaction Models*, book chapter in "Analyzing Multiscale Phenomena Using Singular Perturbation Methods", Proceedings of Symposia in Applied Mathematics, Vol. 56, AMS Short Course (1998). pp. 151-184.